

Two Dimensional Modeling and Inversion of the Acoustic Wave Equation in Inhomogeneous Media

John Fawcett

Abstract

In this paper we outline a fast and efficient method for the finite difference calculation of solutions to the two dimensional acoustic wave equation in an inhomogeneous medium. We then implement our forward modeling scheme in an inversion procedure to determine the two dimensional velocity variation. A numerical example is given.

Introduction

The initial-boundary value problem that is central to the work in this paper is:

$$\frac{1}{c^2(x,z)} \frac{\partial^2 P}{\partial t^2} - \nabla^2 P = \delta(\vec{X} - \vec{X}_0) S(t) \quad (1a)$$

$$P(x, z=0, t) = 0 \quad (1b)$$

$$\frac{\partial P}{\partial z}(x, z=L, t) = 0 \quad (1c)$$

$$P(x, z, t=0) = 0 \quad P_t(x, z, t=0) = 0 \quad (1d)$$

$$S(t) = 0 \quad t < 0 \quad \vec{X}, \vec{X}_0 \in \mathbf{R} \times [0, L] \quad (1e)$$

In terms of acoustics, (1b) represents a pressure release surface and (1c) a rigid bottom. However, the methods which we shall describe, apply equally as well for other choices of boundary conditions (1b) and (1c).

The inverse problem is the estimation of $c(x, z)$ from a knowledge of $\frac{\partial P}{\partial z}(x, z=0, t; \vec{X}_0)$ where \vec{X}_0 represents the source position. In our inversion method we shall parametrize $c(x, z)$ in terms of bicubic splines. The unknown parameters, \vec{p} , will be the values of $c(x, z)$

at the splines' nodes. We shall suppose that we have a set of discrete observations, $\vec{d} \equiv \frac{\partial P}{\partial z}(x_i, z=0, t_j; \vec{X}_0)$. Our method will be a straight-forward implementation of non-linear least squares theory:

$$\min_{\vec{p}} \| \vec{d}_{ij} - L(\vec{p}) |_{i,j} \|_2 \quad (2)$$

where L is the solution of (1). The non-linear least squares algorithm we shall employ is equivalent to solving a sequence of linearized least squares problems. Hence, our method is an iterative application of a linearized method. Tarantola [9] has previously discussed in theory such methods.

At each iteration we must solve the problem (1) for the current estimate of $c(x, z)$, and in fact, we sometimes solve (1) several times to calculate an approximate Jacobian $\frac{\partial L(\vec{p})}{\partial \vec{p}}$. Hence, our forward modeling algorithm must be fast and accurate. We shall first discuss the details of our finite difference modeling program, and then discuss our inversion procedure.

Finite Difference Modeling of the Acoustic Wave Equation

We consider (1) on a finite domain $x \in [0, X]$ $z \in [0, L]$, and we discretize (1) in space and time to obtain the following explicit scheme:

$$\begin{aligned} P^{n+1}(x_i, z_j) - 2P^n(x_i, z_j) + P^{n-1}(x_i, z_j) = & \frac{c^2(x_i, z_j)}{12} r^2 \times \\ & (16(P^n(x_{i+1}, z_j) + P^n(x_i, z_{j+1}) + P^n(x_{i-1}, z_j) + P^n(x_i, z_{j-1}))) \\ & - (P^n(x_{i+2}, z_j) + P^n(x_i, z_{j+2}) + P^n(x_{i-2}, z_j) + P^n(x_i, z_{j-2}))) \\ & - 5c^2(x_i, z_j)r^2 P^n(x_i, z_j) + S(t_n)\delta(l, m)c^2(x_i, z_j)r^2 + O(h^4 + (\Delta t)^2) \end{aligned} \quad (3)$$

$\delta(i, j) = 1$ if $i=l, j=m$: $=0$ otherwise.

We have taken the x and z discretizations both equal to h and $r = \frac{\Delta t}{h}$, where Δt is the time discretization. The Courant-Friedrich-Lewy (CFL) condition for the stability of the scheme (3) is that $r c \leq (\frac{3}{8})^{\frac{1}{2}}$ (Alford et al [1]), where we will take $c \geq \max_{i,j} c(x_i, z_j)$. As is indicated in (3) our scheme is spatially fourth order accurate. The source function $S(t)$ in (1a) determines which wavelengths will dominate in the solution $P(x, z, t)$. A rule of thumb suggested by Alford et al [1] is that for the discretization (3), five grid points per upper half

power wavelength are needed to properly resolve the solution. Here the upper half-power wavelength refers to the upper wavelength $\lambda = \frac{c}{f}$, where the source's power spectrum $|S(f)|^2$ has reached half its maximum value.

The only unusual term in (3) is the source term $S(t_n)\delta(l,m)c^2(x_i,z_j)r^2$. Previous authors have suggested more complicated procedures for the inclusion of sources, but the straightforward inclusion of the source at a single grid point works perfectly well. Intuitively, if the source point \vec{X}_0 is located at the grid point (l,m) then from the discretization of (1a), we would expect the discretized source to have the form:

$$\frac{1}{N}(S(t_n)\delta(l,m)c^2(x_i,z_j)(\Delta t)^2) \quad (4)$$

where N is some normalization. From the definition of a two dimensional delta function $\delta(\vec{X}-\vec{X}_0)$ we know that :

$$(\delta,\Psi(\vec{X})) = \Psi(\vec{X}_0) \quad \text{where} \quad (5a)$$

$$(\delta,\Psi) \equiv \int_0^X \int_0^L \delta(\vec{X}-\vec{X}_0)\Psi(\vec{X})dydx. \quad (5b)$$

A consistent inner product to use with our grid is :

$$(f,g) \equiv \sum_i \sum_j h^2 f(i,j) g(i,j) \quad (6)$$

If we take $\delta(\vec{X}-\vec{X}_0)$ as approximated by $\frac{\delta(l,m)}{N}$, then N must be equal to h^2 for (6) to be consistent with (5a) and (5b). With $N=h^2$, we obtain the source term in (3). We can evaluate $P(x,z,t;\vec{X}_0)$ analytically for $S(t) = t(t-t_c); 0 \leq t \leq t_c$, $S(t)=0 \ t \geq t_c$ and $\frac{\partial P}{\partial z}(x,z=0,t)=0$, $c(x,z) \equiv 1$. In Figure 1, we show the analytical solution for the first arrival, and the numerical solution using scheme (3). Here we are looking at a trace a distance, $|\vec{X}-\vec{X}_0| = .2864$ and we used a grid of 101×51 points with 400 time steps ($\Delta x = \Delta y = .02$, $\Delta t = .005$). (There are two traces here, but they are indistinguishable.)

To implement (3) on the array processor (Floating Point AP 120B) we consider (thanks to Peter Mora) the discrete Laplacian in (3) as a sum of convolutions in the x and z directions. We define the vector \vec{b} :

$$\vec{b} \equiv \left[\frac{-r^2}{12}, \frac{16r^2}{12}, -2.5r^2, \frac{16r^2}{12}, \frac{-r^2}{12} \right] \quad (7)$$

and we can write that :

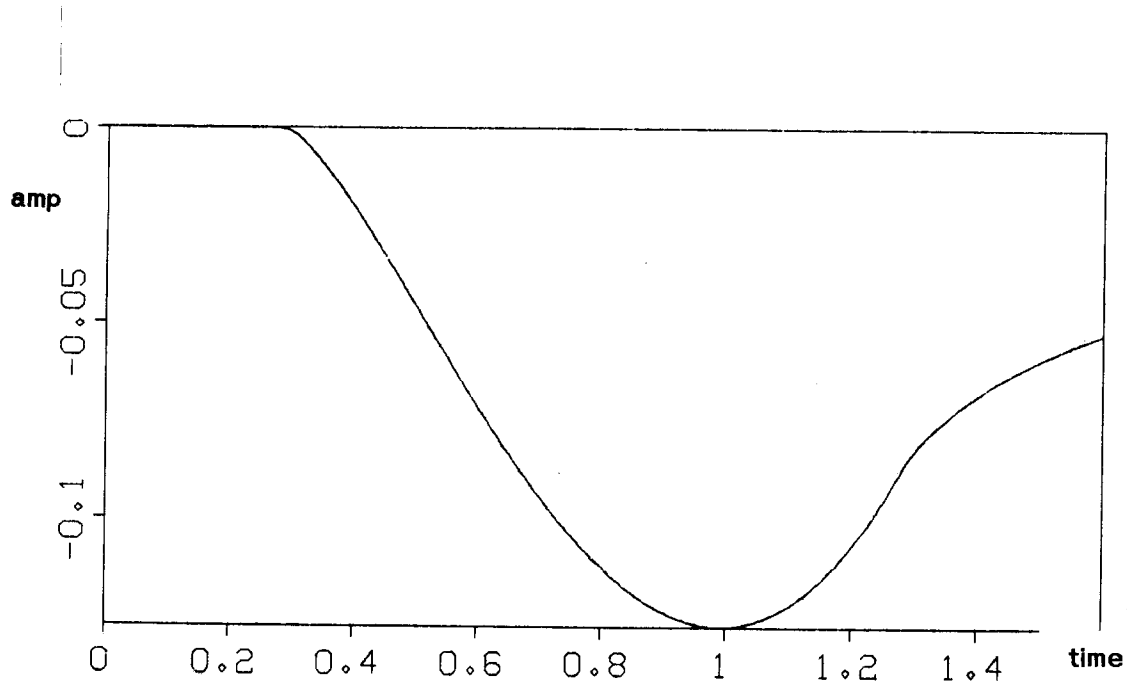


Figure 1. Analytic and Numerical Response to Source $t_c = 1$

$$\nabla^2_{i,j} = \vec{b}(j) * P(i,j) + \vec{b}(i) * P(i,j) \quad (8)$$

This convolution, and all vector/matrix operations are done quickly in the array processor. The field resulting from this convolution is then multiplied by the corresponding elements of the velocity matrix (actually, square of the velocity) to produce \tilde{P} . Then \tilde{P} , P^n , P^{n-1} , and the source contribution for the particular time level are added together to produce P^{n+1} . We then move the elements of P^{n+1} corresponding to the values of the pressure field at selected traces at $z = \Delta z$ into a storage area in the array processor. P^{n-1} is then overwritten by P^n , P^n overwritten by P^{n+1} , and we start again for the next time step. This whole procedure, for all time steps, is carried out with one call to the array processor. For a small grid (e.g., 51×26 with 200 time steps) we have a saving of a factor of 8 to 10 times over the VAX, using the array processor; for larger grids the savings is even more substantial. At the end of all the time steps, we transfer $P(x_j, z = \Delta z, t)$ to the VAX, and use $\frac{P(x_j, z = \Delta z, t)}{\Delta z}$ to represent $\frac{\partial P}{\partial z}(x_j, z = 0, t)$.

Finally, we must address the question of implementing boundary conditions. Our boundary conditions in the vertical direction (1b) and (1c) have physical significance and are easy to implement. We can consider our grid to have 2 rows appended to the top, and 2 rows appended to the bottom. We then simply extend the solution oddly and evenly, respectively, about the two boundaries. However, in our finite domain, the horizontal boundaries have no physical significance, but numerically we must impose some boundary condition. Many authors have suggested various **absorbing boundary conditions** which in some way simulate a transparent boundary. Clayton and Engquist [3] have given schemes based upon one-way wave operator approximations. Here the accuracy (in particular the range of incident angles over which the approximation is valid) and the complexity of the scheme depends upon the order of the one-way operator used

In our problems, energy will be reflected off the top and bottom boundaries and there will be in general, energy incident upon the side boundaries at a large range of incident angles. Also, although probably possible to implement in the array processor, we desire, for our first attempts at inversion, simple boundary conditions which can be easily **internally** implemented. A "brute force" method is to make the horizontal size of the grid large enough so that reflections from the sides would have no effect on the traces of interest in the relevant time window. However, due to storage limitations within the array processor, we cannot make the grid too large. Our method is to use a grid twice as large horizontally as vertically, and we then calculate the pressure field twice, once for zero boundary conditions on the sides and once for zero-slope conditions. We then average the two solutions (see also Smith [8]). This effectively gives us a grid four times as wide as deep. Perhaps in the future, we shall examine the more effective use of side boundary conditions.

Optimization Procedure

As we mentioned above, we will assume that $c(x,z)$ is parametrizable in terms of bicubic splines. This is most suited for the situation where $c(x,z)$ is smooth. The use of one-dimensional spline approximations for one-dimensional inverse problems has previously been studied by Banks et al [2]. The algorithm we use for two dimensional spline interpolation is based on that of de Boor [4]. Here, we suppose we have a grid with $c_{i,j}$ the value of $c(x,z)$ at $x=x_i, z=z_j$. Then one dimensional cubic splines are found in the x and z directions. This procedure determines $\frac{\partial c}{\partial x}$ and $\frac{\partial c}{\partial z}$ at the nodes. Fitting bicubic splines along each column of the grid (or row) determines $\frac{\partial^2 c}{\partial x \partial z}$ at the node points. The 4 quantities $\left(c_{i,j}, \frac{\partial c_{i,j}}{\partial x}, \frac{\partial c_{i,j}}{\partial z}, \frac{\partial^2 c_{i,j}}{\partial x \partial z} \right)$ at 4 corners uniquely determines the bicubic spline

$\varphi(x, z) \equiv \sum_{m=0}^3 \sum_{n=0}^3 \Gamma_{m,n}^{i,j} (x-x_i)^m (z-z_j)^n$ within the rectangle bounded by the corners. With the one-dimensional splines, there is always the problem of what to do at the boundaries. We used de Boor's [5] "not-a-knot" condition. This is a condition that replaces the need for derivative information at the endpoints with a condition that requires the two cubics on the last 2 intervals to have continuous third derivative at their common node (i.e., they are the same cubic).

The parameters, \vec{p} , to determine are the values of $c(x, z)$ at the nodes. Once we have found $c(x, z)$ at the nodes, then from bicubic spline interpolation, $c(x, z)$ is known everywhere, within this approximation. Our problem is :

$$\min_{\vec{p}} \|\vec{d} - L(\vec{p})\|_2 \quad (9)$$

We will employ the Gauss-Newton method for non-linear least squares. If we denote $\vec{d} - L(\vec{p})$ as \vec{F} and $\Phi(\vec{p}) \equiv \frac{1}{2} \vec{F}^T \vec{F}$ then (9) is equivalent to finding \vec{p}_0 such that $\nabla \Phi = \vec{0}$ where \vec{p}_0 is a minimum point. To find \vec{p}_0 , Newton's method would be:

$$\vec{p}^{n+1} = \vec{p}^n + \Delta \vec{p}^n \quad \text{where:} \quad (10)$$

$$\Delta \vec{p}^n = \left[-\nabla^2 \Phi \right]^{-1} \nabla \Phi(\vec{p})$$

For problems, where $\vec{F}(\vec{p}_0) \approx \vec{0}$, then the Gauss-Newton method approximates $\nabla^2 \Phi$ by $\underline{J}^T \underline{J}$ where :

$$J_{i,j} \equiv \frac{\partial F_i}{\partial p_j} \quad i=1, \dots, m \quad j=1, \dots, n$$

Thus, we can write (10) as:

$$\Delta \vec{p}^n = \left[-\underline{J}^T \underline{J} \right]^{-1} \underline{J}^T \vec{F}(\vec{p}) \quad (11)$$

The vector, $\Delta \vec{p}^n$, is also the solution of the linear least squares problem

$$\min_{\vec{p}} \|\underline{J} \Delta \vec{p} + \vec{F}\|_2 \quad (12)$$

It is often advantageous to "damp" the step of (11), and use instead :

$$\Delta \vec{p}^n = - \left[\underline{J}^T \underline{J} + \lambda_n I \right]^{-1} \underline{J}^T \vec{F}(\vec{p}) \quad (13)$$

Now $\Delta \vec{p}$ is the solution of the linear minimization problem with the following coefficient matrix :

$$\begin{matrix} \mathbf{m} \\ \mathbf{n} \end{matrix} \begin{bmatrix} \underline{J} & -\vec{F} \\ \lambda_n I & \vec{0} \end{bmatrix} \tag{14}$$

Our choice of λ_n will be such that $\|\vec{F}^{n+1}\|_2 < \|\vec{F}^n\|_2$. For λ_n sufficiently large, this condition will be true, as $\Delta\vec{p}$ becomes aligned with $-\nabla\Phi(\vec{p})$ for $\lambda_n \rightarrow \infty$. To find the minimal length solution of (14), we employed Golub's [6] QR method of solution. We employed it once to reduce (14) to the form:

$$\begin{matrix} \mathbf{m} \\ \mathbf{n} \end{matrix} \begin{bmatrix} \underline{T} & -Q\vec{F} \\ \lambda_n I & \vec{0} \end{bmatrix} R_1 \tag{15}$$

where \underline{T} is upper triangular, and then storing R_1 , we repeatedly solve (15) (usually once or twice) to find a good choice of λ_n (see Osborne [7]).

Another method of solution of (13) is using the singular value decomposition of the matrix \underline{J} :

$$\underline{J} = \underline{U} \underline{\Lambda} \underline{V}^T \tag{16}$$

Here, $\underline{\Lambda}$ is a diagonal matrix containing the singular values of \underline{J} . The columns of \underline{V} (the eigenvectors of $\underline{J}^T \underline{J}$) corresponding to small singular values, represent the portion of parameter space which cannot be resolved in a stable fashion. We will sometimes use (16) at our last iteration to determine what portions of the velocity field are not "well" determined.

Having the data vector, \vec{d} as input to our inversion problem, and calculating $L(\vec{p})$ using our finite difference method, it is easy to calculate the residual vector \vec{F} . However, we must also calculate the Jacobian matrix $\frac{\partial \vec{F}}{\partial \vec{p}}$. Tarantola [9] has discussed such calculations. His method is based upon the linearization of the wave operator. If we write $n(x,z) = \frac{1}{c^2(x,z)} = n^0(x,z) + \epsilon n^1(x,z)$ and $P = P^0 + \epsilon P^1$ where P^0 is the wave solution for the slowness field n^0 , then we obtain:

$$\begin{aligned} n^0 P^0_{tt} + n^0 \epsilon P^1_{tt} + \epsilon n^1 P^0_{tt} \\ + \nabla^2 P^0 + \epsilon \nabla^2 P^1 = \delta(\vec{X} - \vec{X}_0) S(t) + O(\epsilon^2) \end{aligned} \tag{17}$$

Hence,

$$P^1(\vec{X}, t) = -\int G^0(\vec{X}, t; \vec{X}') * P^0_{tt}(\vec{X}', t) n^1(\vec{X}') d\vec{X}' \tag{18}$$

or:

$$\frac{\delta P}{\delta \vec{p}} = - \int G^0(\vec{X}, t; \vec{X}') * P^0_{tt}(\vec{X}', t) \delta n(\delta \vec{p}) d\vec{X}'$$

Here * denotes convolution in time and G^0 is the unperturbed Green's function. Whether to use (18) as a formula for the computation of the Frechet derivative depends upon the geometry of the problem under consideration. In general, we would have to numerically calculate $G(\vec{X}, t; \vec{X}_s)$. This would mean a wavefield calculation for various source positions \vec{X}_s . The judicious use of a reciprocity relation could reduce the amount of calculation: however a large amount of computation still remains. On the other hand, if the data consists of the pressure field for many different source positions, then using (18) may indeed be appropriate.

We will usually be considering in our inversion examples single shot data, with various receiver positions. For these problems, it is more efficient to perturb \vec{p} and form $\vec{p}' = \vec{p} + \varepsilon \vec{e}_j$ where $\vec{e}_j = [0, 0, \dots, 1, \dots, 0]^T$ (the "1" in the j'th position) and recalculate the wavefield. Hence,

$$\frac{\partial f_i}{\partial p_j} = \frac{F_i(\vec{p}') - F_i(\vec{p})}{\varepsilon} + O(\varepsilon) \quad (19)$$

Numerical Examples

Example 1

For this example the source is located at a horizontal distance of 2.5 km. and at a depth of .3 km. The velocity field was $c(x, z) = 1.5 \times (1 + 0.2 \sin(12x) \times \sin(12z)) \text{ km/s}$. To generate the synthetic data, we did the finite difference calculations completely within the VAX with a grid size of 501 horizontal points, 51 depth points, and 400 time steps with $\Delta t = .0025$. Our source function was $S(t) = .5 H(t) e^{-1000(t-.15)^2}$. The Fourier Transform, $\tilde{S}(\omega)$ defined as $\int_{-\infty}^{\infty} S(t) e^{-i\omega t} dt$ is approximately equal to $.5 \sqrt{\frac{\pi}{1000}} e^{\frac{-\omega^2}{4000}} e^{.15i\omega}$. This is a broadband source which has half-power at about 6 Hz. Using $c \approx 1.5 \text{ km/s}$, then the half-power wavelength is $\lambda \approx .25 \text{ km}$. Thus we are, from the rule discussed above, using a sufficient number of grid points.

For the inversion we shall use for data, traces from 16 offsets : $x_i = .02 + (i-1) \times .06$ $i = 1, \dots, 16$,with 50 time samples, $t_j = .25 + .01 \times (j-1)$ $j = 1, \dots, 50$ for each of these traces. This data for all 401 time samples is shown in Figure 2. For the finite difference scheme in the inversion , we use a coarser grid than in the data generation; we use 51 horizontal points and 26 vertical points. However, we still use 400 time steps, so that during the iterations the velocity can increase to approximately 5 km/sec without the CFL stability requirement being violated.

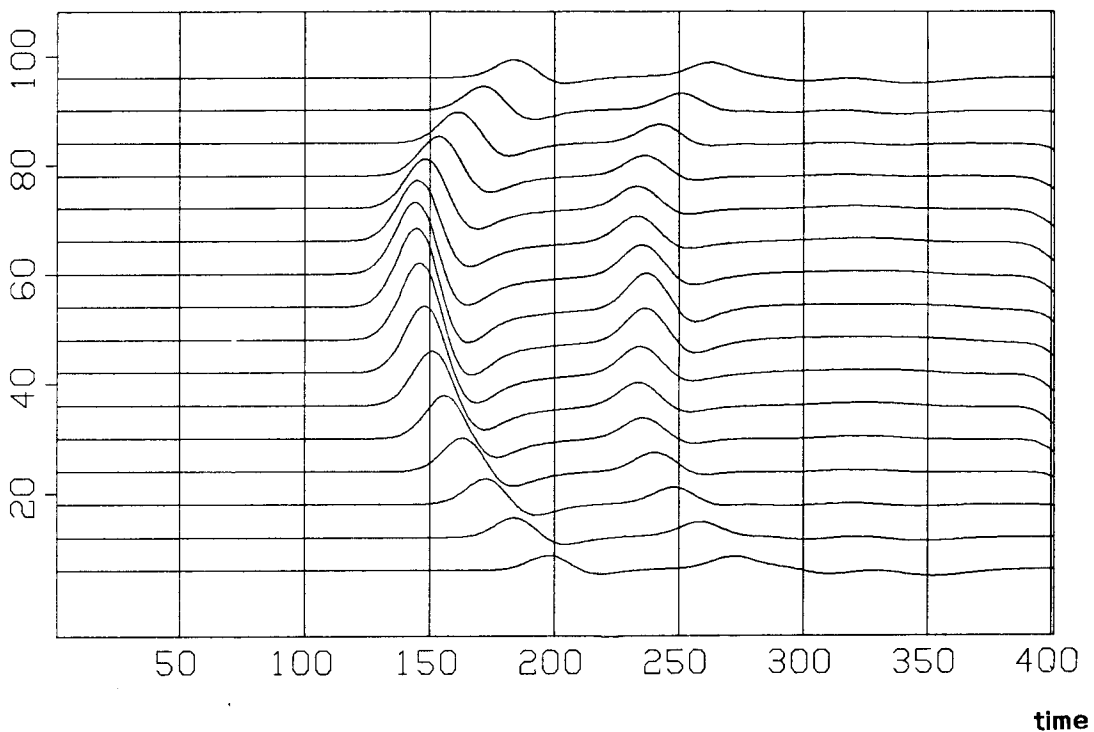


Figure 2. The Sixteen Traces used for Inversion

Along the top row, we will assume that the velocity is known; it is 1.5 km/s . We will have 18 parameters to determine. We take as an initial guess : $c_{ij}(i=1,6 j=2,4) = 1.6 \text{ km/s}$. In this run, we did not allow λ_n to fall below 1. In Figure 3 we show a comparison of the input data and calculated data sets for the initial guess. In Table 1 , we show the residual $\|\vec{F}\|_2$, and the magnitude of the gradient vector $\|\underline{J}^T \vec{F}\|_2$

at each iteration. We also show the resulting velocity field at selected iterations in Figure 4a-4d. In Figure 4e, we plot the true field $c(x,z)$ for comparison. The values of c_{ij} , after the final iteration are given in Table 2. In Figure 5, we show the data and calculated fields after the second iteration.

it	$\ \vec{F}\ _2$	$\ \underline{J}^T \vec{F}\ _2$
1	9.30004	141.865
2	4.16730	52.5459
3	2.36897	47.1720
4	1.74593	16.3310
5	1.53574	6.23639
6	1.46706	1.32478
7	1.43601	0.47162
8	1.41921	0.30535
9	1.40903	0.23679

The final residual, for the velocity estimate after the ninth iteration was $\|\vec{F}\|_2 = 1.401723$.

1	2	3	4	5	6
1.500	1.500	1.500	1.500	1.500	1.500
0.752	1.647	1.307	1.402	1.522	0.824
1.861	1.030	1.738	1.908	1.003	2.172
1.579	1.832	1.462	0.905	1.335	1.439

We note that the true and inverted velocity fields qualitatively agree. However, it was necessary to use $\lambda_n \equiv 1$ throughout the calculation as otherwise "wild" estimates for the nodes in the outer portions of the grid were obtained. Simple ray considerations, using our source and receiver locations, show that very little energy propagates through these portions of the grid. Thus, indeed, this portion of the velocity field is not well constrained from the data. We note that the 4 vertical node points determine one cubic interpolant. We show this cubic, determined by the inversion, and the true vertical profile for the centre trace ($n_x = 26$) in Figure 6.

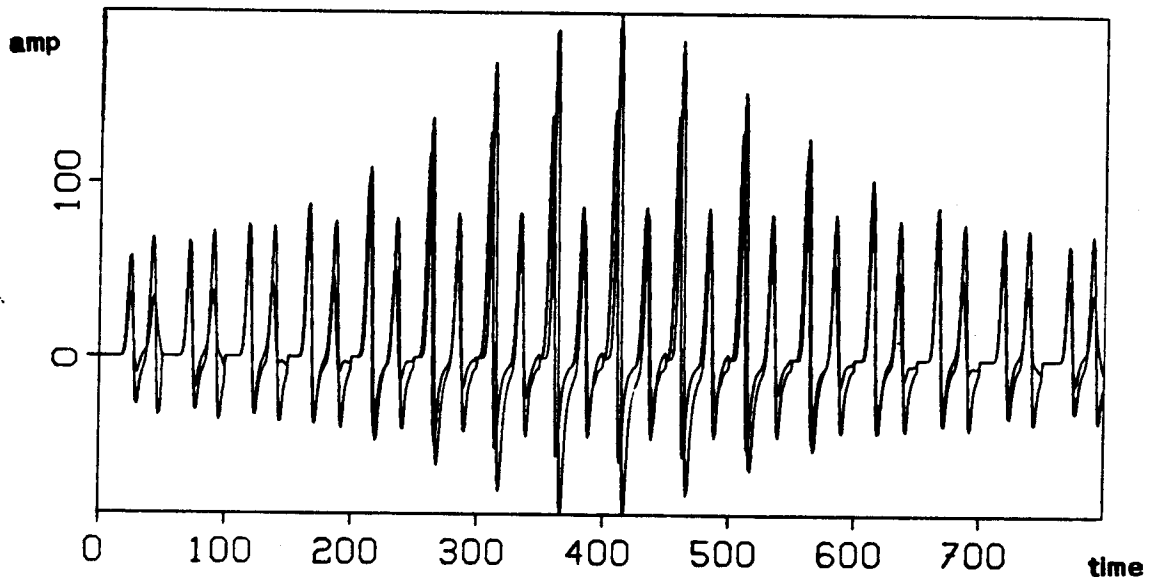


Figure 3. Discretized Data and the Generated Data for Initial Guess

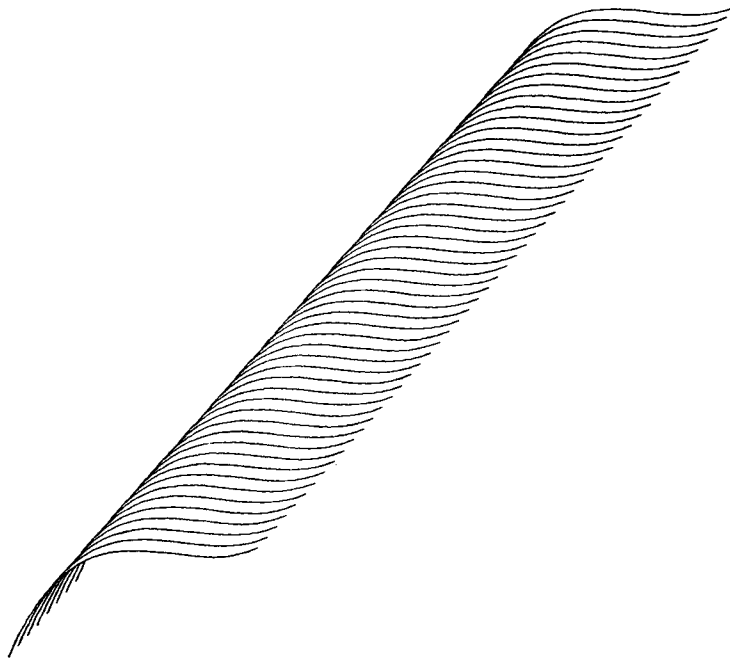


Figure 4a. Initial Velocity Field ($-1.5\text{km} / \text{s}$)

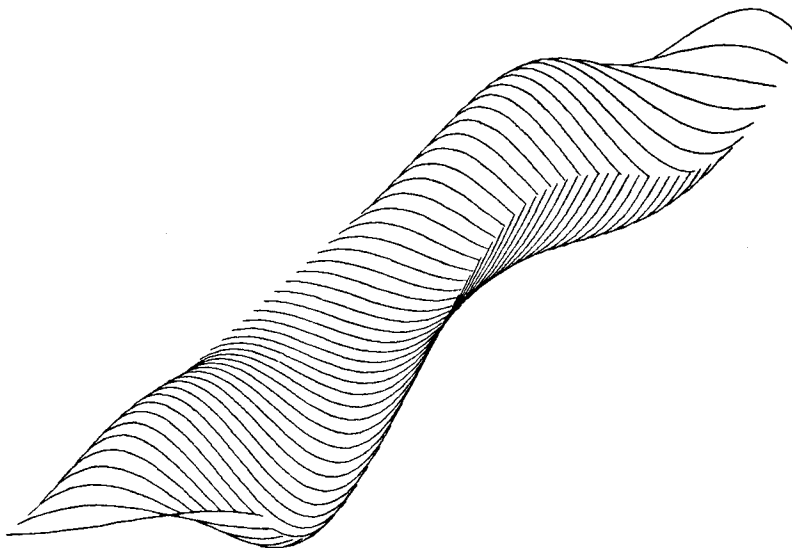


Figure 4b. Velocity Field After First Iteration

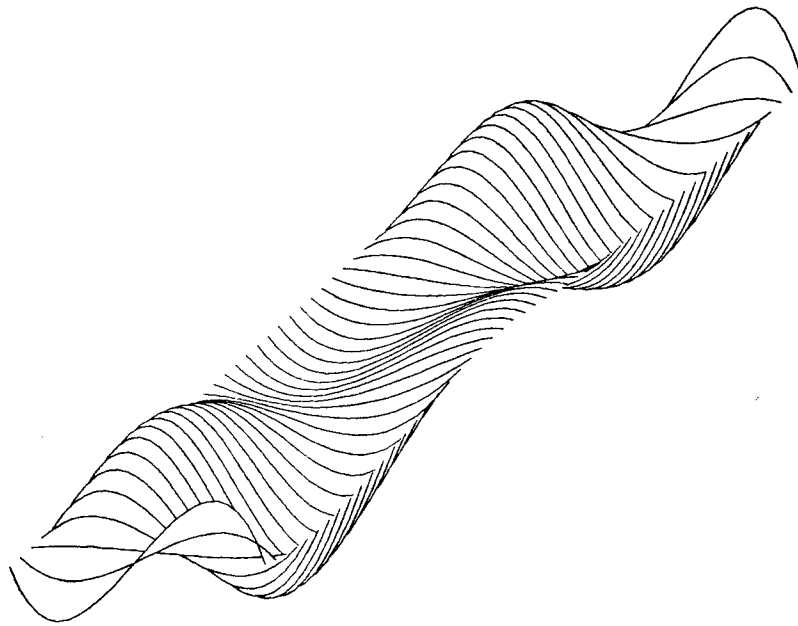


Figure 4c. Velocity Field After Second Iteration

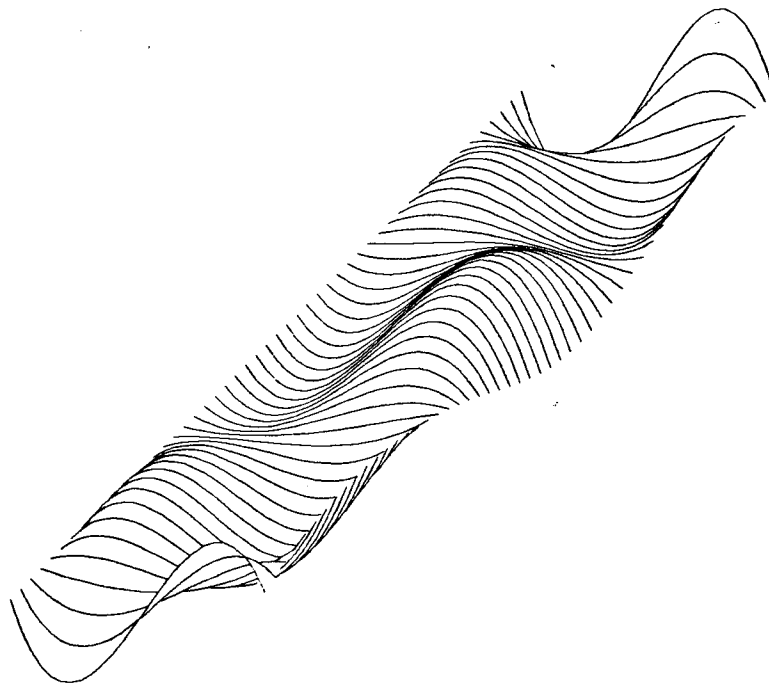


Figure 4d. Velocity Field After Final Iteration

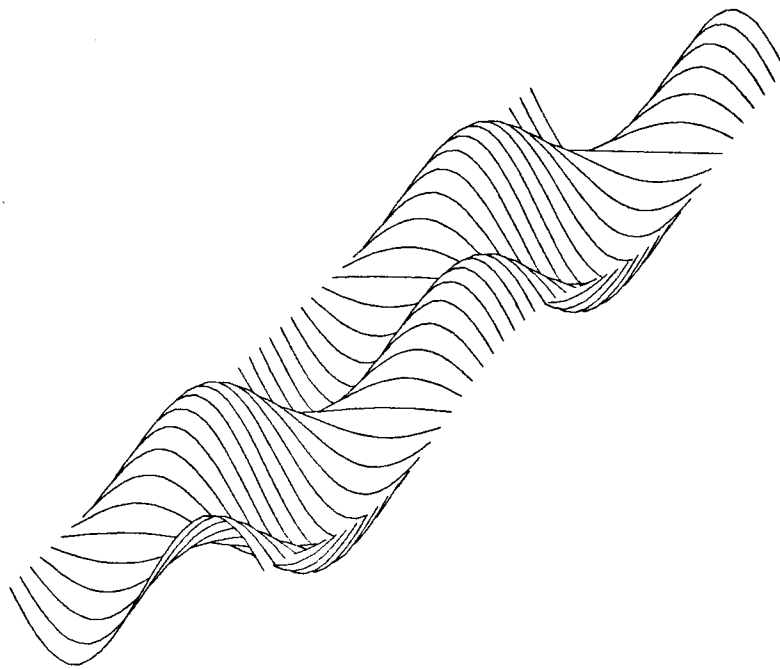


Figure 4e. True Perturbation to the Field (1.5km / s)

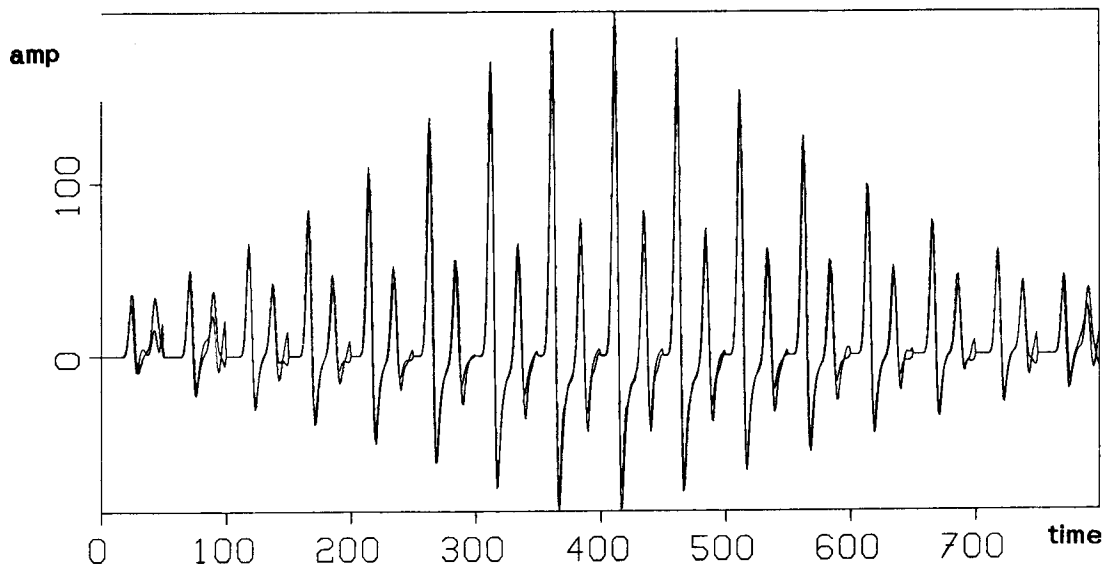


Figure 5. Discretized Data and Generated Data After Second Iteration

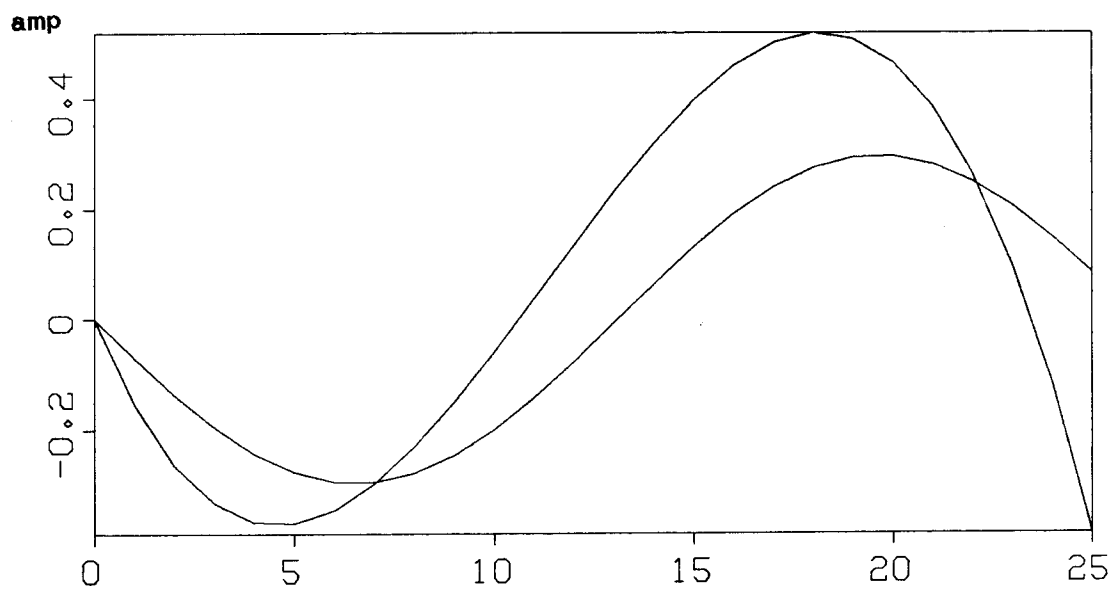


Figure 6. True and Approximate Vertical Profile for Centre Trace

Acknowledgements

I would like to thank Peter Mora and Dr. Chris Anderson of the Departments of Mathematics and Computing Science for some very helpful discussions. Also, I would like to thank Professor Joseph Keller of the Department of Mathematics for his critique of an earlier version of this report. Financial support for my tenure at Stanford comes from the Air Force Office of Scientific Research, the Army Research Office, the Office of Naval Research, and the National Science Foundation.

References

- [1] R.Alford, K.Kelly, and D.Boore., "Accuracy of Finite-Difference Modeling of the Acoustic Wave Equation", **Geophysics**, 39,No.6, P.834-842 (1974).
- [2] H.Banks, K.Ito, and K.Murphy., "Computational Methods for Estimation of Parameters in Hyperbolic Systems", **ICASE Report**, (Sept. 1983).
- [3] R.Clayton and B.Engquist., "Absorbing Boundary Conditions for Acoustic and Elastic Wave Equations", **B.S.S.A.**, 67,No.6.,p.1529-1540 (1977).
- [4] C.de Boor., **A Practical Guide to Splines**. Applied Mathematical Sciences, 27, Springer-Verlag, New York (1978).
- [5] C. de Boor., "Bicubic Spline Interpolation", **J. Math. Phys.** ,41,p.212-218 (1962).
- [6] G.Golub., "Numerical Methods for Solving Linear Least Squares Problems", **Numerische Mathematik** ,7,p206-216 (1965).
- [7] M.Osborne., "Some Aspects of Non-Linear Least Squares Calculations", **Conference on Numerical Methods for Non-Linear Optimization**. ,University of Dundee, 1971 (ed. F.A.Lootsma), Academic Press, London, p.171-191 (1972).

- [8] W.Smith., " A Non-Reflecting Plane Boundary For Wave Propagation Problems", **J. Comp Physics** ,15,p.492-503 (1974).
- [9] A.Tarantola., "Nonlinear Inverse Problem For an Heterogeneous Acoustic Medium", preprint (1983).

Total = 387241	817 function	445 table	293 count
31454 the	816 error	438 left	290 non
11196 of	801 any	433 before	290 lisp
11007 is	774 commands	428 point	288 way
10882 to	770 terminal	425 like	288 just
8340 and	730 more	424 call	288 free
6868 in	725 should	422 special	286 numbers
4512 be	722 current	417 where	285 version
4467 for	721 but	410 following	282 language
4106 are	719 other	408 make	281 integer
4044 file	717 read	408 control	277 etc
3541 if	715 process	403 such	276 long
3345 by	682 these	395 information	276 causes
3158 it	681 given	394 array	276 beginning
3078 this	668 description	391 thus	274 made
2836 or	663 example	389 entry	272 blocks
2813 as	654 end	381 code	271 through
2709 on	649 than	380 device	267 available
2673 that	649 string	377 printed	266 compiler
2659 with	649 into	377 mail	264 zero
2393 not	648 new	377 functions	261 group
2287 you	645 default	376 page	259 begin
2159 name	642 standard	376 editor	256 order
2094 which	641 do	375 most	253 start
2064 an	612 directory	370 form	253 open
2057 line	591 must	368 length	252 values
1962 command	584 so	366 would	252 edit
1869 will	573 shell	349 single	252 disk
1628 can	569 two	346 signal	251 found
1449 from	559 its	346 right	251 contains
1405 system	556 expression	345 tape	251 address
1392 files	552 up	344 macro	249 normally
1391 number	550 argument	344 buffer	249 level
1384 may	544 mode	339 source	246 instead
1331 used	543 after	336 second	245 returned
1326 input	541 print	335 word	244 stack
1308 one	537 unix	333 trace	241 above
1299 at	533 arguments	333 change	239 useful
1292 output	525 was	331 options	237 both
1224 when	525 out	331 bugs	236 their
1188 all	520 they	327 bytes	236 named
1136 character	518 format	326 between	236 common
1107 program	516 been	324 get	235 messages
1096 also	515 same	324 called	233 run
1082 then	512 some	323 now	233 memory
1058 have	511 last	322 returns	233 flag
1036 list	506 section	322 possible	232 executed
1015 no	505 block	320 what	230 prints
986 see	504 message	319 header	230 nil
980 each	501 write	317 about	229 manual
973 text	501 size	313 since	228 followed
971 use	500 specified	313 another	227 double
970 first	496 we	311 define	227 contents
949 set	491 programs	309 written	225 field
943 lines	486 synopsis	309 done	225 described
929 there	483 does	307 char	224 users
921 data	480 space	306 statement	223 over
901 has	474 case	298 them	223 editing
900 user	470 next	298 include	222 changed
865 only	469 your	297 symbol	221 want
860 type	469 return	297 many	221 result
847 time	463 using	296 while	221 processes
832 characters	460 option	296 variable	220 otherwise
822 value	448 names	293 machine	220 defined